

## DOUBLE GAMMA-RAY LINES FROM UNASSOCIATED FERMI-LAT SOURCES

MENG SU<sup>1,\*</sup>, DOUGLAS P. FINKBEINER<sup>1,2</sup>

*Draft version May 6, 2018*

### ABSTRACT

Gamma ray emission from dark matter subhalos in the Milky Way has long been sought as a sign of dark matter particle annihilation. So far, searches for gamma-ray continuum from subhalos have been unsuccessful, and line searches are difficult without prior knowledge of the line energies. Guided by recent claims of line emission at 111 and 129 GeV in the Galactic center, we examine the coadded gamma-ray spectrum of unassociated point sources in the Second *Fermi*-LAT catalog (2FGL) using 3.9 years of LAT data. Using the SOURCE event class, we find evidence for lines at 111 GeV and 129 GeV with a local significance of  $3.3\sigma$  based on a conservative estimate of the background at  $E > 135$  GeV. Other 2FGL sources analyzed in the same way do not show line emission at 111 and 129 GeV. The line-emitting sources are mostly within 30 degrees of the Galactic plane, although this anisotropy may be a selection effect. If the double-line emission from these objects is confirmed with future data, it will provide compelling support for the hypothesis that the Galactic center line signal is indeed from dark matter annihilation.

*Subject headings:* gamma rays — line emission — milky way — dark matter

### 1. INTRODUCTION

Although a wide variety of cosmological and astrophysical observations provide compelling evidence that nonbaryonic dark matter constitutes  $\sim 80\%$  of the total matter in the Universe, we still know little about its nature (e.g. Bergström 2012; Hooper & Profumo 2007; Bertone et al. 2005).

In many models of weakly interacting massive particle (WIMP) dark matter, particles annihilate and/or decay to gamma rays directly or indirectly. Gamma-ray photons at energies  $E \gg 1$  GeV travel in straight lines without significant energy losses in the local Universe, allowing their spatial distribution to serve as a tracer of the dark matter distribution. Regions of high dark matter density such as the Galactic center, galaxy clusters, and dwarf galaxies have been suggested as possible sources. In addition, many DM subhalos in the MW may shine in gamma rays and have no counterpart at other wavelengths, making them promising sources (see recently e.g. Belikov et al. 2011; Ackermann et al. 2012b; Mirabal et al. 2012, and references therein)

The primary challenge in such searches is to understand the background from conventional astrophysics well enough to distinguish a dark matter signal. A “smoking-gun” signal of annihilating dark matter would be the discovery of one or more gamma-ray lines. The line(s) could be produced by dark matter decays or annihilations into two photons, or two-body final states

involving one photon plus a Higgs boson, Z boson, or other chargeless non-SM particle. No plausible astrophysical background can produce a line, although a narrow feature is possible (see Aharonian et al. 2012). In most models, the line flux is suppressed by a loop factor relative to the continuum, implying it is 2-3 orders of magnitude fainter (e.g. Bergström & Ullio 1997). Although this is not true in all models (e.g. Bergström et al. 1998; Bergström 2000; Bertone et al. 2009; Jackson et al. 2010; Cline 2012), this theoretical prejudice led previous studies to focus on continuum searches. However, tentative evidence for gamma-ray line emission at  $\sim 130$  GeV toward the inner Galaxy has been found with  $3.3\sigma$  significance after trials factor<sup>4</sup> correction (Weniger 2012).

In our recent paper (Su & Finkbeiner 2012b), we have performed a study with various data analysis methods and obtained  $6.5\sigma$  local significance of the gamma-ray study with various data analysis methods and obtained  $6.6\sigma$  local significance of the gamma-ray line structure, and  $5.0$ - $5.5\sigma$  after trials factor (depending on whether we assume one line or two lines). In fact, we found *two* lines centered at 111 GeV and 129 GeV provide a better fit to the data.

The high significance of this result does not address concerns about instrumental artifacts, such as energy mapping errors that could give rise to spectral bumps and dips (Finkbeiner et al. 2012). Such concerns must be addressed by an independent analysis of photons from other parts of the sky. For example, detection of lines at 111 and 129 GeV elsewhere on the sky in multiple unassociated LAT sources, but *not* in any class of associated LAT sources would rule out an energy mapping error in

<sup>1</sup> Institute for Theory and Computation, Harvard-Smithsonian Center for Astrophysics, 60 Garden Street, MS-51, Cambridge, MA 02138 USA

<sup>2</sup> Center for the Fundamental Laws of Nature, Physics Department, Harvard University, Cambridge, MA 02138 USA

\* mengsu@cfa.harvard.edu

<sup>4</sup> Also known as the “look elsewhere effect”

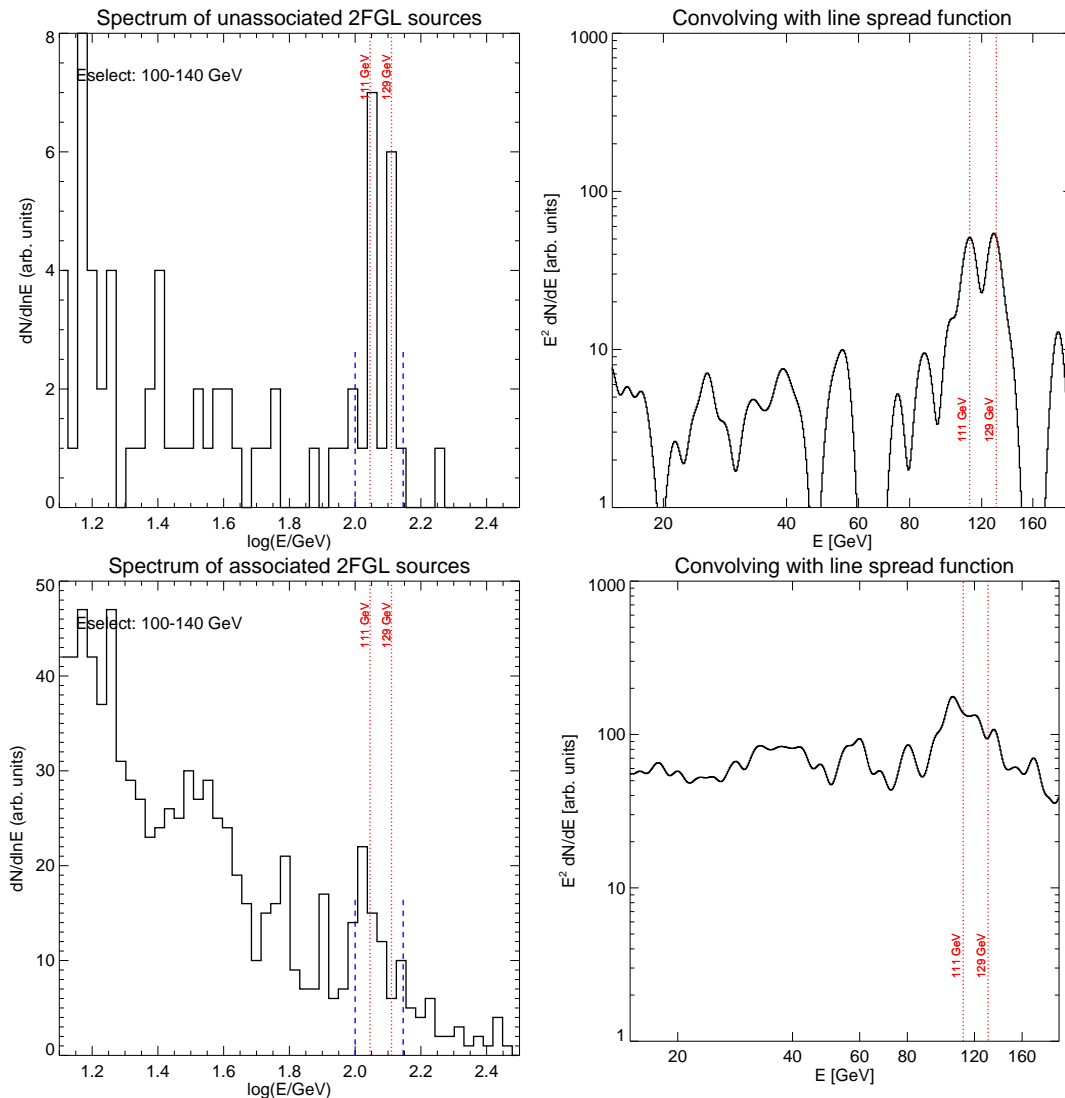


FIG. 1.— Upper left: the spectrum of 16 unassociated point sources in the 2FGL catalog, chosen to have a photon at  $E = 100 - 140$  GeV (vertical blue lines). The photons are drawn from the SOURCE event class in 3.9 years of data, with a match radius of  $0.15/0.3^\circ$  for FRONT/BACK converting events. The expected energies (red vertical lines) and histogram binning (black) are identical to our previous paper on the Galactic center (Su & Finkbeiner 2012b). The upper right panel is the same spectrum after convolving with the LAT line spread function (Rajaraman et al. 2012) and multiplying by  $E$ . The lower two panels are the same as the upper two panels, but for associated point sources. The associated source spectrum shows a bump between the blue lines due to the strong selection bias, but shows no evidence for a doublet at the expected energies.

the LAT data processing as a source of the Galactic center lines. Even a lower significance detection would be interesting, because there is no trials factor for choice of line energies.

Many of the *Fermi*-LAT point sources are associated with counterparts at other wavelengths, including blazars (BL Lacs, Flat Spectrum Radio Sources (FSRS), etc.), other AGNs (Seyferts, Radio Galaxies, etc.), pulsars and binaries, and other Galactic sources (Nolan et al. 2012). Although substantially improved over the First *Fermi*-LAT catalog (Abdo et al. 2010a), there are still 344 sources in the 2FGL ( $\sim 15\%$  of the total) without obvious counterparts at Galactic latitude  $|b| \geq 5^\circ$ .

Various statistical methods and theoretical scenarios have been suggested to classify and explain these

unassociated sources (Ackermann et al. 2012a), including the existence of new types of source classes, e.g. dark matter subhalos. Numerical simulations suggest that within the Milky Way halo, dark matter subhalos form at all mass scales down to the simulation resolution. Less massive halos might show themselves as gamma-ray sources without significant emission at other wavelengths (Belikov et al. 2011; Ackermann et al. 2012b; Buckley & Hooper 2010). If such a signal were detected, it would be the first non-gravitational signature of dark matter.

In this work, we use 3.9 years of LAT data to study the gamma-ray spectrum of the unassociated point sources in the 2FGL catalog to search for gamma-ray *line emission*. We find that the energy spectrum shows two lines at 111

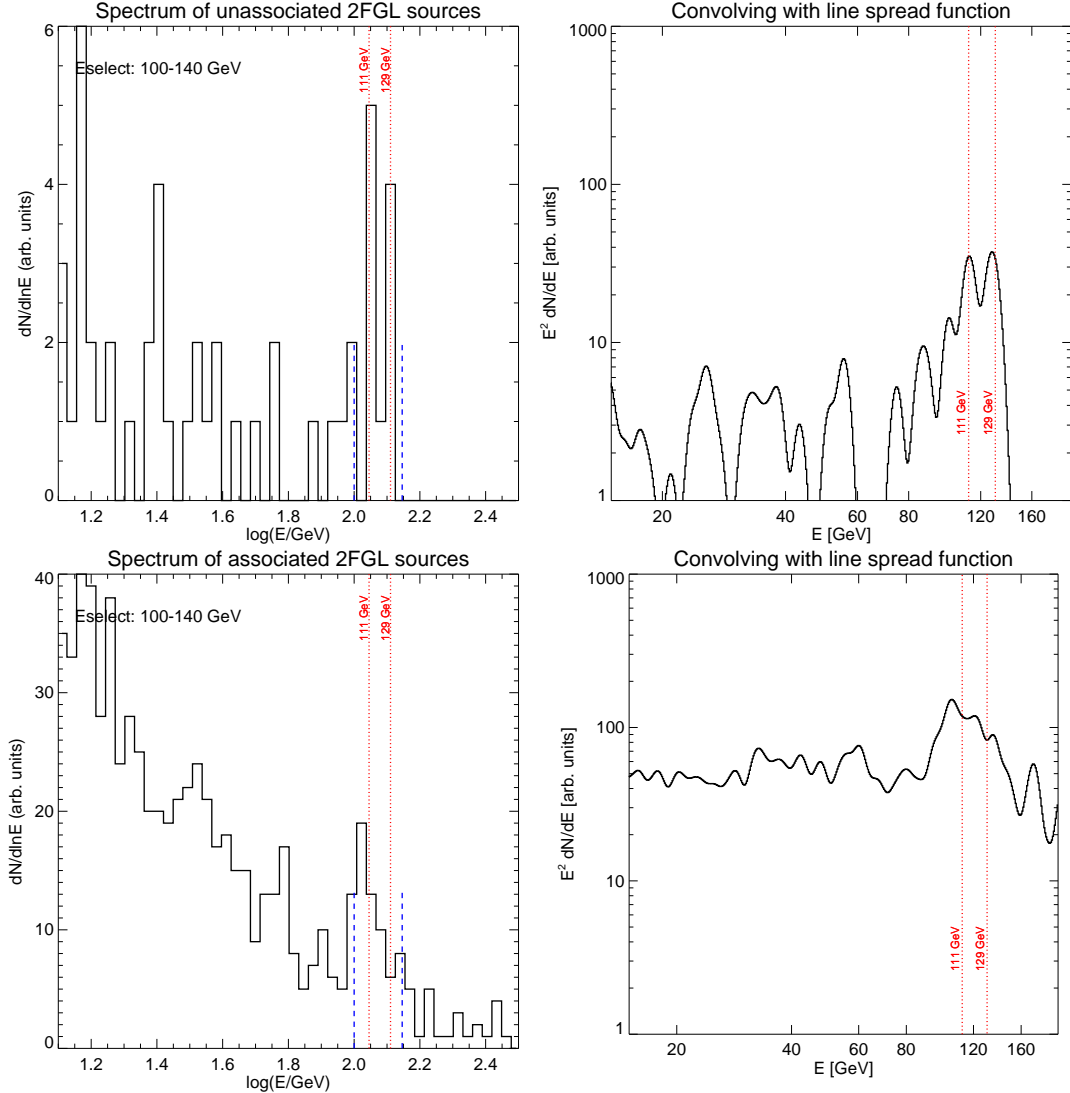


FIG. 2.— Same as Figure 1, but using the ULTRACLEAN event class.

GeV and 129 GeV. In Section 2 we describe our LAT data selection and analysis procedure. In Section 3 we examine the spectral line emission by various statistical tests and we summarize our main findings in Section 4.

## 2. FERMI DATA SELECTION

In this section, we briefly describe our data selection and analysis procedure. We refer to our previous papers for more detailed information (Su et al. 2010; Su & Finkbeiner 2012a,b). The *Fermi* LAT is a pair-conversion telescope, in which incoming photons convert to  $e^+e^-$  pairs, which are then tracked through the detector. The arrival direction and energy of each event are reconstructed, and the time of arrival recorded. The LAT is designed to survey the gamma-ray sky in the energy range from about 20 MeV to several hundreds of GeV. The point spread function (PSF) is about  $0.8^\circ$  for 68% containment at 1 GeV and decreases with energy as  $r_{68} \sim E^{-0.8}$ , asymptoting to  $\sim 0.2^\circ$  at high energy. It is convenient to distinguish between front-converting

and back-converting events that convert in the front and back regions of the tracker, respectively. The 68% containment radius at high energy is  $r_{68} \sim 0.15^\circ$  for front-converting and  $r_{68} \sim 0.30^\circ$  for back-converting events, with some dependence on the incidence angle on the detector.

The LAT energy resolution (i.e. the half-width of the 68% containment region) is of order 10% over most of the energy range (see Fermi-LAT Collaboration 2012, for details). Around 100 GeV, the resolution is closer to 7% for high incidence-angle events, and twice that for normal incidence.

We use the latest publicly available data and instrument response functions, known as Pass 7 (P7\_V6)<sup>5</sup>. We perform our analysis on both SOURCE and ULTRACLEAN events, and present figures based on each for comparison. The former has larger effective area and higher

<sup>5</sup> Details at [http://fermi.gsfc.nasa.gov/ssc/data/analysis/documentation/Pass7\\_usage.html](http://fermi.gsfc.nasa.gov/ssc/data/analysis/documentation/Pass7_usage.html)

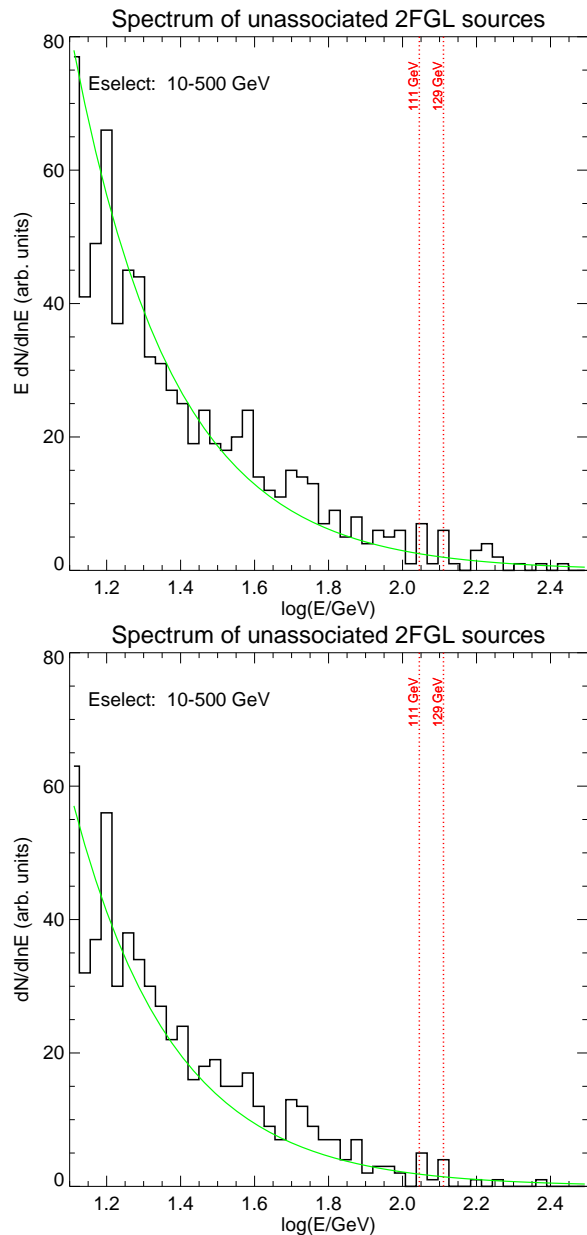


FIG. 3.— Upper panel: same as the upper left panel of Figure 1 (with an extra power of  $E$ , but for all unassociated sources. The green line is a power law  $dN/dE \sim E^{-2.6}$  fit to events at  $E > 135$  GeV. Lower panel: same but for ULTRACLEAN class. The suspicious bump at  $\log E = 2.2$  in the upper panel disappears in the lower panel. However, the background estimate in the lower panel appears to be unreasonably low, so the green line is multiplied by a factor of 2.5 to match the lower energy emission. Because of this disagreement, we do not use the ULTRACLEAN data for our final result.

background. At the energies of interest CLEAN and ULTRACLEAN events give identical results.

Photons coming from the bright limb at Earth’s horizon, dominantly produced by grazing-incidence CR showers in the atmosphere, are a potential source of contamination. We remove this background by selecting events with zenith angle less than  $105^\circ$ . We also exclude some time intervals when data quality is poor, primarily while *Fermi* passes through the South Atlantic Anomaly.

### 3. ANALYSIS

High resolution simulations suggest the existence of hierarchical dark matter halo structures on all resolved mass scales (e.g. Kuhlen et al. 2009; Pieri et al. 2008). The high end of the mass function is visible in the Milky Way as dwarf galaxies, including the Magellanic clouds. Less massive subhalos could be too small to contain enough baryonic matter to be visible at other wavelengths, but shine only via annihilation of dark matter particles in gamma rays. Such sources may appear as unassociated *Fermi*-LAT sources in the 2FGL catalog, which forms the basis for our line search.

#### 3.1. Source selection

The *Fermi*-LAT 2FGL catalog consists of 1873 sources (100 MeV-100 GeV), of which 1290 are firmly identified/associated and 575 (31%) are unassociated sources (Nolan et al. 2012). Cutting to Galactic latitude  $|b| > 5^\circ$  to avoid contamination from the Galactic disk results in 344 unassociated sources. Since dark matter emission is expected to be non-variable in time, we also remove the 25 among the 344 unassociated sources which have been flagged with `variability_index`  $> 41.6$ . Then we select photon events with energy in the range 100-140 GeV and zenith angle less than  $105^\circ$ . We include both FRONT and BACK converting events. Among the remaining 319 unassociated sources we select ones with at least one 100-140 GeV photon within  $0.15^\circ/0.3^\circ$  for FRONT/BACK converting events, which results in 16 unassociated sources for SOURCE event class. The detailed information of these 16 sources can be found in Table 1.

In Nolan et al. (2012), it has been noted that 51% of the unassociated sources have been flagged due to various issues (compared to 14% of the associated sources). We have tried cutting on each flag bit and find no significant impact on our results. In order to avoid introducing an additional trials factor, we decided not to cut on any flags.

#### 3.2. Composite energy spectrum

We show the energy spectrum of the regions within  $0.15^\circ/0.3^\circ$  for FRONT/BACK converting events in two ways. In the left panels of Figure 1 and 2, we show the photon counts binned in  $\log E$ . The binning used is the same as in Fig. 16 of Su & Finkbeiner (2012b). This binning was chosen to optimize the signal on the 111 GeV and 129 GeV lines in the Galactic center, and has *not* been modified for this study. In the right panels of Figure 1, we plot  $E^2 dN/dE$  for the unbinned event distribution convolved with the line-spread function (LSF) (Edmonds 2011; Su & Finkbeiner 2012b). Each of these representations has pros and cons. The histograms make it easy to see how many photons contribute to each bin, and allow simple computations of Poisson likelihoods. The unbinned spectra give a sense of the spectrum without any

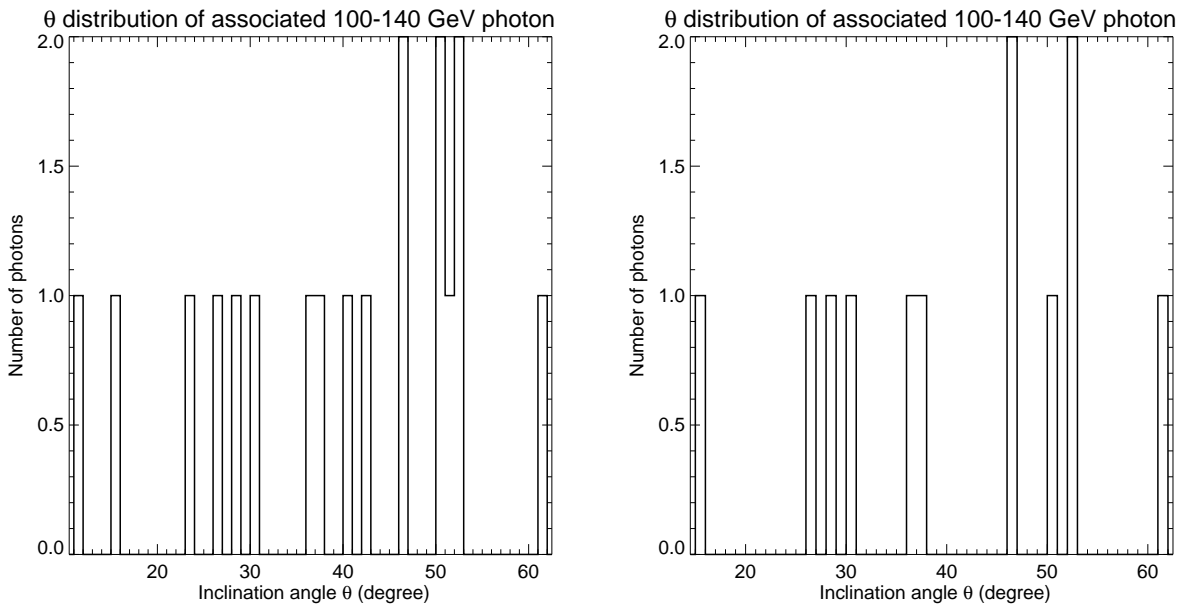


FIG. 4.— The inclination angle distribution of the 100-140 GeV photons in left panels of Figure 1 and Figure 2, i.e. for SOURCE and ULTRACLEAN events, respectively.

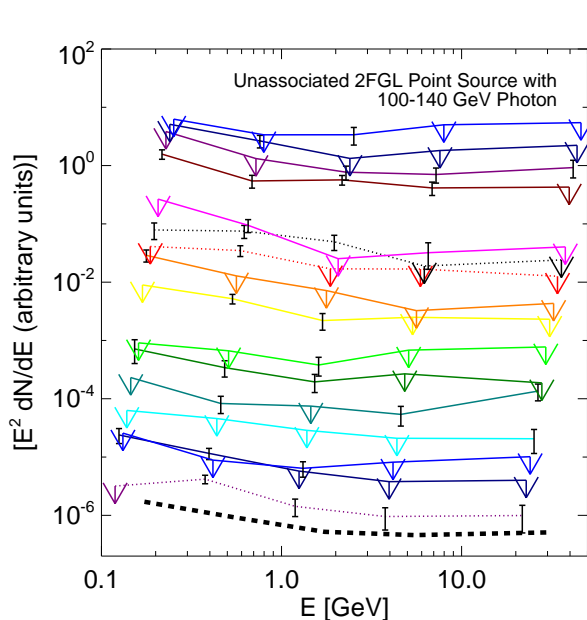


FIG. 5.— The energy spectrum of unassociated 2FGL sources which have a 100-140 GeV photon within  $0.15^\circ/0.3^\circ$  radius for FRONT/BACK LAT events. The spectrum is obtained from the 2FGL catalog. Sources thought to be potentially confused with Galactic diffuse emission are shown with dotted lines. The dashed black line shows the average of all the spectra. Each band shows integral photon flux from [0.1-0.3, 0.3-1, 1-3, 3-10, 10-100] GeV respectively from the likelihood analysis in that band with fixed photon power-law index. A  $2\sigma$  upper limit is shown if the source is not significant in a band.

arbitrary binning choices, and convolution by the LSF allows maximum sensitivity to faint signals. However, the spectrum is “twice convolved” (once by the instrument and once by the processing) making the lines blend together to an undesirable degree. In the following we use the binned histograms for analysis, and provide the

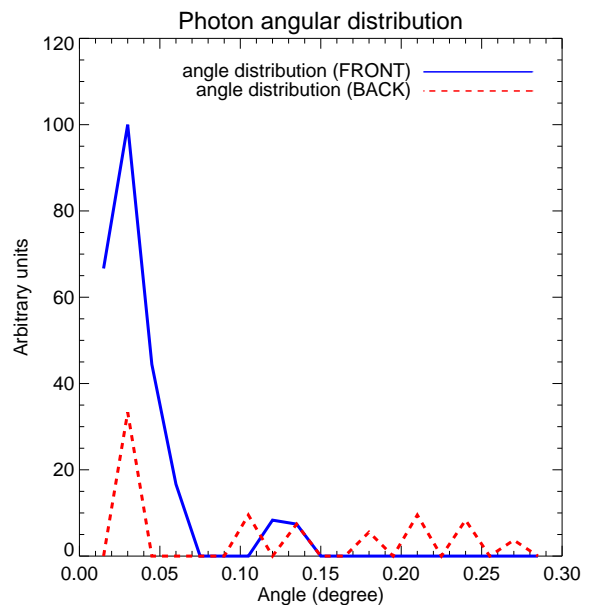


FIG. 6.— The angular distribution of 100-140 GeV photons matching with unassociated 2FGL sources within  $0.15^\circ/0.3^\circ$  radius for FRONT/BACK LAT events (shown with solid/blue and dash/red curve, respectively). The distribution is normalized by the annular area given a radius. The FRONT events shows more concentrated distribution than the BACK events, consistent with the expectation based on the point spread function. Both FRONT and BACK events suggest a central concentrated distribution.

smoothed spectra only for reference.

We plot the energy spectrum for photons near the 16 unassociated sources with a photon at 100-140 GeV for SOURCE (Figure 1) and ULTRACLEAN (Figure 2) event classes. While this selection obviously suppresses the spectrum outside of the 100-140 GeV range, there is no way it can rearrange photons in the 100-140 GeV win-

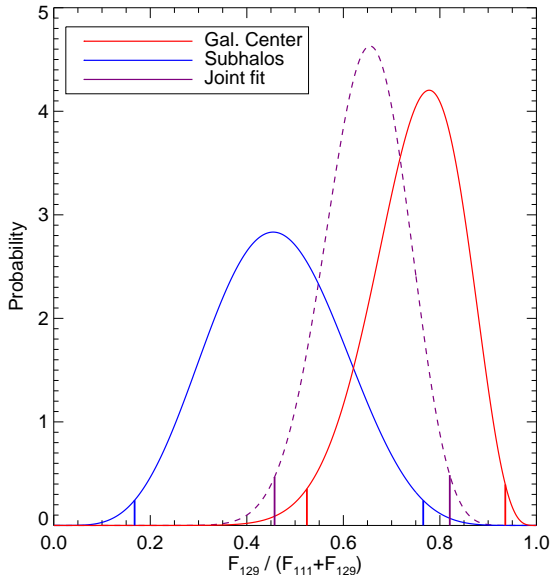


FIG. 7.— Probability of obtaining the observed counts, in the energy bins centered on 111 and 129 GeV, in the Galactic center and subhalos as a function of the line fraction  $f \equiv F_{129}/(F_{111} + F_{129})$ . We find that the best fit ratio of the 129 GeV line to 111 GeV line is 1.5, and the  $2\sigma$  range of the line ratio is [0.84, 4.5]. See Section 3.6 for details.

dow. Intriguingly, we find two gamma-ray emission lines at 111 GeV and 129 GeV. One interpretation is that unassociated sources emit a gamma-ray doublet. Another is that some flaw in the LAT data preferentially maps events to these energies. In order to test this hypothesis, we apply the *same* selection procedure to associated point sources, also shown in Figures 1 and 2, and find no line features at 111 GeV or 129 GeV.

For each of the 16 unassociated sources, we show the integrated photon flux in energy bands (0.1-0.3, 0.3-1, 1-3, 3-10, 10-100) GeV respectively in Figure 5, obtained from the 2FGL catalog. Among the 16 sources, three of them are marked with potentially confused with Galactic diffuse emission.

### 3.3. Statistical significance

Even with low statistics (7 counts at 111 GeV and 6 counts at 129 GeV) it is possible to obtain a significant result if the backgrounds are low enough. Because WIMP annihilations can produce lower energy photons (final-state radiation, Z/W continuum, inverse-Compton, etc.) it may be incorrect to use lower energy emission to assess the background. However, at high energy there are very few photons in these sources, and there would be none from a 129 GeV WIMP. As a compromise, we assume the background is a power law, fit its amplitude to high energy ( $135 < E < 270$ ), but choose the power-law index so that lower energy emission is modeled approximately correctly (Figure 3).

We assess the Poisson probability of observing 13 (or more) SOURCE counts in the two spectral bins with the

background estimate in the upper panel of Figure 3. This has a probability of  $p = 0.00069$  corresponding to  $3.2\sigma$ . Removing sources to be potentially confused with Galactic diffuse emission (marked out in 2FGL) only mildly affect our results ( $3.3\sigma$ ). The ULTRACLEAN events would give a much higher significance ( $> 4\sigma$ ) if we could believe the background estimate, but it looks implausibly low.

### 3.4. Spatial distribution

The subhalo candidates identified in this work are mostly distributed at  $|b| < 20^\circ$ , at all longitudes. It is not clear whether this could be a selection effect, a fluke, or a hint about the true distribution of dark matter subhalos. On one hand, dark matter subhalos preferentially dragged into the Galactic disk may lead to disk-like configurations, e.g. the proposed “dark disk” (e.g. Bruch et al. 2009; Purcell et al. 2009). On the other hand, the distribution is not concentrated in longitude, so they may be nearby subhalos with lower mass, close enough to appear brighter than more massive subhalos, e.g. those hosting dwarf galaxies.

### 3.5. Radial profile

In Figure 6, we show the stacked angular distribution of 100-140 GeV photons, which are selected by matching with unassociated 2FGL sources within  $0.15^\circ/0.3^\circ$  radius for FRONT/BACK LAT events, with respect to the source center provided by 2FGL. The distribution is normalized by the annular area at each radius. The FRONT events show a more concentrated distribution than the BACK events, consistent with the point spread function. Both FRONT and BACK events suggest a centrally concentrated distribution.

### 3.6. Line ratio

Our previous work (Su & Finkbeiner 2012b) found 4 (14) photons above background at 111 (129) GeV. This led us to expect the 129 GeV line might be stronger, but this work finds the 111 GeV to have slightly more counts: 6 (5) at 111 (129) GeV above background. Are these results compatible?

In order to determine a confidence interval for the line ratio, we consider a total of  $N$  photons for the doublet, with  $k$  of them in the 129 GeV bin, and the rest in the 111 GeV bin. The binomial probability of observing  $k$  of  $N$  counts in this bin is

$$P_b(k, n, f) = \frac{N!}{k!(N-k)!} f^k (1-f)^{N-k} \quad (1)$$

where  $f \equiv F_{129}/(F_{111} + F_{129})$  is the true fraction of doublet photons at 129 GeV. Figure 7 shows this probability (i.e., the probability of observing  $k$  counts given  $N$  and  $f$ ) as a function of  $f$  for the GC, subhalos, and the product of the two.

To obtain a confidence interval, we find  $f_{\text{low}}$  such that

$$P(k \geq x, n, f_{\text{low}}) = \sum_{k=x}^N P_b(k, n, f) = 0.025 \quad (2)$$

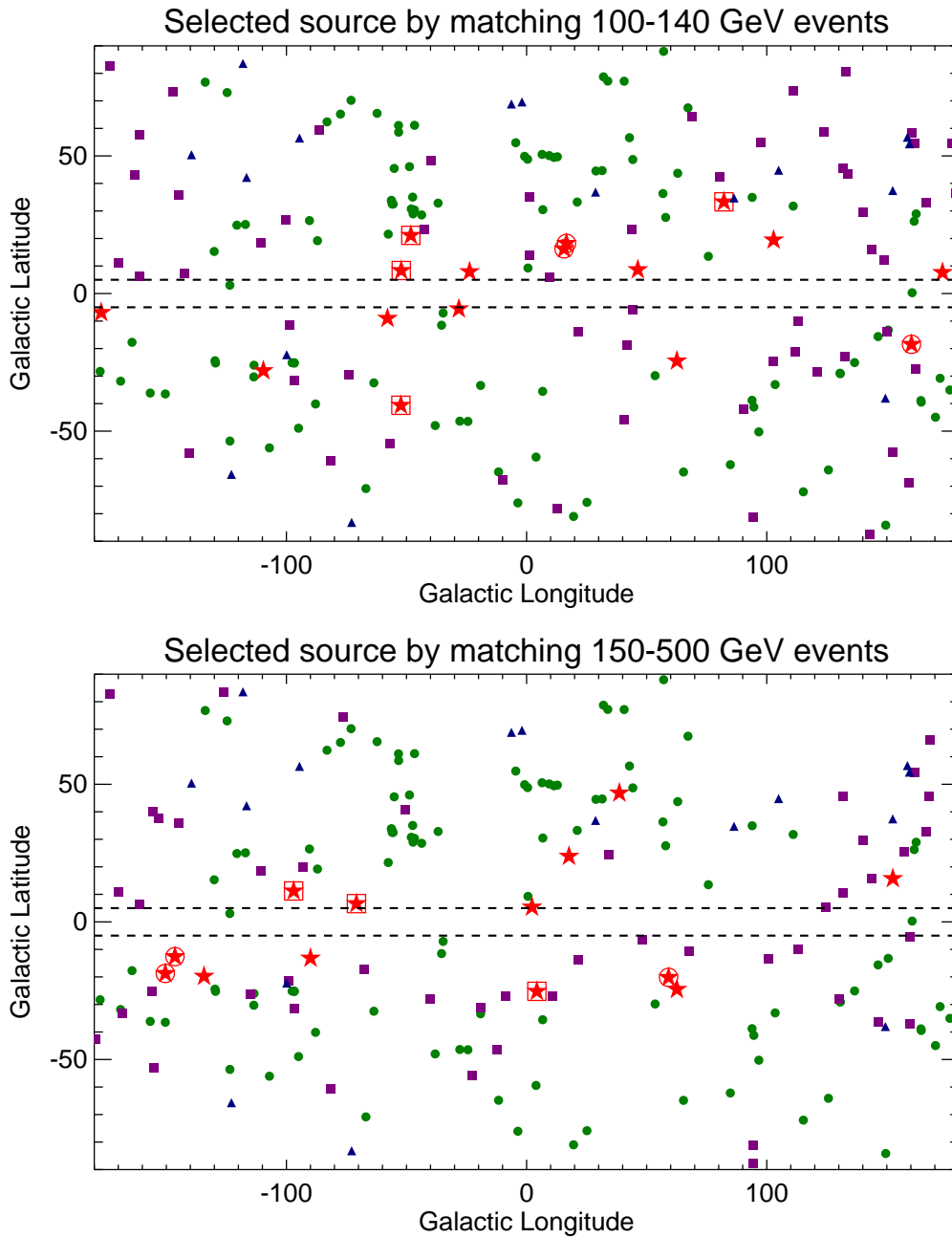


FIG. 8.— The spatial distribution of unassociated 2FGL sources which have a 100-140 GeV photon within  $0.15^\circ/0.3^\circ$  radius for FRONT/BACK LAT events (red stars). For comparison, we also show the spatial distribution of 16 dwarf galaxies (e.g. Abdo et al. 2010b, blue triangles), 106 nearby galaxy clusters (Reiprich & Böhringer 2002, dark green circles), and associated sources with the same matching criteria (purple squares). We find no spatial overlaps between these sources. Unassociated sources thought to be potentially confused with Galactic diffuse emission (red circles) and unassociated sources with less than  $5\sigma$  detection (red squares) are noted. The lower panel shows the same plot as the upper panel but selected unassociated point sources by matching with 150-500 GeV events. In both cases, the sources with high-energy photons are mostly near the disk. This implies that the Galactic latitude distribution may result from a selection effect.

with a complementary expression for  $f_{\text{high}}$ . The 95% confidence interval (corresponding to “ $2\sigma$ ” confidence) is then  $0.167 < f < 0.765$  for the subhalos and  $0.524 < f < 0.935$  for the Galactic center. A significant range of  $f$  is allowed in both cases, so we can combine the counts from both and obtain  $0.457 < f < 0.820$  for the joint fit. This yields 95% confidence bounds on the line ratio  $0.84 < F_{129}/F_{111} < 4.5$ . The data are consistent (at  $2\sigma$ ) with the lines being equally strong, but also with the

129 GeV line being 4.5 times as strong. Clearly more data will be required to measure the line ratio with high confidence.

#### 4. DISCUSSION AND CONCLUSION

In this paper, we have reported evidence for line emission at 111 GeV and 129 GeV from unassociated *Fermi*-LAT point sources. The lines have a significance of  $p = 6.9 \times 10^{-4}$  or  $3.2\sigma$  for a simple power-law background

model. These results provide independent support for our previous claims of a double gamma-ray line in the Galactic center at the *same* energies (Su & Finkbeiner 2012b). The double line emission is compatible with the scenario of a 129 GeV WIMP annihilating to  $\gamma\gamma$  and  $\gamma Z$ , producing the two lines. As a test of systematics, we apply the same selection and analysis procedure to associated *Fermi*-LAT point sources, and find no evidence for lines at these energies. It is difficult to imagine instrumental systematics that could produce this double line emission only at the Galactic center region and the locations of unassociated point sources without affecting other regions of the sky. We find this evidence to be persuasive, but it cannot be considered conclusive until more data become available.

Further observations are essential, not only to firmly establish the existence of the lines, but to measure the line ratio. The ratio of  $\gamma Z$  and  $\gamma\gamma$  line strength depends only on the particle physics model, and is independent of the astrophysical uncertainties such as the dark matter distribution in the halo. The line pair is also compatible with a 141 GeV WIMP annihilating through  $\gamma Z$  and  $\gamma h$  for  $m_h \sim 125$  GeV, as in the ‘‘Higgs in Space’’ scenario (Jackson et al. 2010). However, we have not found any significant gamma-ray line at  $\sim 141$  GeV. In any case, additional data will be critical for measuring the line ratio, which is currently only poorly determined (Figure 7).

A possible change to the *Fermi* scan strategy could accumulate S/N on the double spectral lines in the Galactic center up to  $\sim 4$  times as fast as the current survey strategy, and it is crucial for studying the double line emission. We believe this could be done with only modest impact on other *Fermi* science objectives. With the huge effective area and low energy threshold of H.E.S.S II, it may be possible to confirm a spectral bump in the

Galactic center fairly soon. However, the energy resolution of H.E.S.S. II is inferior to LAT at 129 GeV, and it may be difficult to resolve the doublet.

The 2FGL catalog is based on 24 months of LAT data, and an updated catalog based on 48 months would provide improved source parameters and associations, decreasing the background noise for the subhalo analysis presented here. Furthermore, multi-wavelength follow-up observations would be helpful to identify the nature of unassociated 2FGL sources and refine the list of associations.

By stacking the unassociated 2FGL point sources together, it might be possible to reveal the spatial profile of the gamma-ray distribution at 111 GeV and 129 GeV. One may in principle improve the positional information of these unassociated sources by using high energy photons and better quantifying the gamma-ray spatial profile. However, with  $\sim 1$  photon per source at high energy, the details of the algorithm used for centroiding the sources are critical, and consideration of the spatial profile is beyond the scope of this work. We simply use the position provided by the *Fermi* 2FGL catalog.

**Acknowledgments:** We thank Christoph Weniger, Dan Hooper, and Neal Weiner for helpful conversations. We acknowledge the use of public data from the *Fermi* data archive at <http://fermi.gsfc.nasa.gov/ssc/>. This work would not be possible without the work of hundreds of people, over many years, to design, build, and operate *Fermi*. M.S. and D.P.F. are partially supported by the NASA Fermi Guest Investigator Program. This research made use of the NASA Astrophysics Data System (ADS) and the IDL Astronomy User’s Library at Goddard (Available at <http://idlastro.gsfc.nasa.gov>).

## REFERENCES

- Abdo, A. A. et al. 2010a, *ApJS*, 188, 405, 1002.2280  
 —. 2010b, *ApJ*, 712, 147, 1001.4531  
 Ackermann, M. et al. 2012a, *ApJ*, 753, 83, 1108.1202  
 —. 2012b, *ApJ*, 747, 121, 1201.2691  
 Aharonian, F., Khangulyan, D., & Malyshev, D. 2012, *ArXiv e-prints*, 1207.0458  
 Belikov, A. V., Hooper, D., & Buckley, M. R. 2011, *ArXiv e-prints*, 1111.2613  
 Bergström, L. 2000, *Reports on Progress in Physics*, 63, 793, [arXiv:hep-ph/0002126](http://arxiv.org/abs/hep-ph/0002126)  
 —. 2012, *ArXiv e-prints*, 1205.4882  
 Bergström, L., & Ullio, P. 1997, *Nuclear Physics B*, 504, 27, [arXiv:hep-ph/9706232](http://arxiv.org/abs/hep-ph/9706232)  
 Bergström, L., Ullio, P., & Buckley, J. H. 1998, *Astroparticle Physics*, 9, 137, [arXiv:astro-ph/9712318](http://arxiv.org/abs/astro-ph/9712318)  
 Bertone, G., Hooper, D., & Silk, J. 2005, *Phys. Rep.*, 405, 279, [arXiv:hep-ph/0404175](http://arxiv.org/abs/hep-ph/0404175)  
 Bertone, G., Jackson, C. B., Shaughnessy, G., Tait, T. M. P., & Vallinotto, A. 2009, *Phys. Rev. D*, 80, 023512, 0904.1442  
 Bruch, T., Read, J., Baudis, L., & Lake, G. 2009, *ApJ*, 696, 920, 0804.2896  
 Buckley, M. R., & Hooper, D. 2010, *Phys. Rev. D*, 82, 063501, 1004.1644  
 Cline, J. M. 2012, *ArXiv e-prints*, 1205.2688  
 Edmonds, Y. V. 2011, PhD thesis, Stanford University  
 Fermi-LAT Collaboration. 2012, *ArXiv e-prints*, 1206.1896  
 Finkbeiner, D. P., Su, M., & Weniger, C. 2012, in preparation  
 Hooper, D., & Profumo, S. 2007, *Phys. Rep.*, 453, 29, [arXiv:hep-ph/0701197](http://arxiv.org/abs/hep-ph/0701197)  
 Jackson, C. B., Servant, G., Shaughnessy, G., Tait, T. M. P., & Taoso, M. 2010, *JCAP*, 4, 4, 0912.0004  
 Kuhlen, M., Madau, P., & Silk, J. 2009, *Science*, 325, 970, 0907.0005  
 Mirabal, N., Frías-Martínez, V., Hassan, T., & Frías-Martínez, E. 2012, *MNRAS*, 424, L64, 1205.4825  
 Nolan, P. L. et al. 2012, *ApJS*, 199, 31, 1108.1435  
 Pieri, L., Bertone, G., & Branchini, E. 2008, *MNRAS*, 384, 1627, 0706.2101  
 Purcell, C. W., Bullock, J. S., & Kaplinghat, M. 2009, *ApJ*, 703, 2275, 0906.5348  
 Rajaraman, A., Tait, T. M. P., & Whiteson, D. 2012, *ArXiv e-prints*, 1205.4723  
 Reiprich, T. H., & Böhringer, H. 2002, *ApJ*, 567, 716, [arXiv:astro-ph/0111285](http://arxiv.org/abs/astro-ph/0111285)  
 Su, M., & Finkbeiner, D. P. 2012a, *ArXiv e-prints*, 1205.5852  
 —. 2012b, *ArXiv e-prints*, 1206.1616  
 Su, M., Slatyer, T. R., & Finkbeiner, D. P. 2010, *ApJ*, 724, 1044, 1005.5480  
 Weniger, C. 2012, *ArXiv e-prints*, 1204.2797



TABLE 1

Source name	RA	Dec	$\ell$	b	Flags	$\sigma$	Variability	Spec index	Radius	Spec type
2FGL J0341.8+3148c	55.5	31.8	160.3	-18.4	32	7.6	24.7	$2.31 \pm 0.09$	0.0706	PowerLaw
2FGL J0526.6+2248	81.7	22.8	182.9	-6.9	1	7.1	27.5	$2.88 \pm 0.16$	0.0641	PowerLaw
2FGL J0555.9-4348	89.0	-43.8	250.4	-28.0	0	5.0	29.1	$2.11 \pm 0.17$	0.0994	PowerLaw
2FGL J0600.9+3839	90.2	38.7	173.2	7.6	0	5.1	14.1	$2.04 \pm 0.21$	0.0490	PowerLaw
2FGL J1240.6-7151	190.2	-71.9	302.1	-9.0	0	8.2	18.4	$1.82 \pm 0.16$	0.0458	PowerLaw
2FGL J1324.4-5411	201.1	-54.2	307.8	8.4	24	4.9	23.3	$2.39 \pm 0.14$	0.1126	PowerLaw
2FGL J1335.3-4058	203.8	-41.0	311.8	21.1	0	4.6	11.2	$2.13 \pm 0.18$	0.0800	PowerLaw
2FGL J1601.1-4220	240.3	-42.3	336.3	7.9	0	7.3	20.8	$2.46 \pm 0.10$	0.1037	PowerLaw
2FGL J1639.7-5504	249.9	-55.1	331.8	-5.6	9	5.9	21.1	$2.79 \pm 0.14$	0.0568	PowerLaw
2FGL J1716.6-0526c	259.2	-5.4	16.6	18.2	2080	6.8	25.7	$2.43 \pm 0.26$	0.1052	LogParabola
2FGL J1721.5-0718c	260.4	-7.3	15.6	16.2	41	6.0	20.9	$2.68 \pm 0.36$	0.0795	LogParabola
2FGL J1730.8+5427	262.7	54.5	82.2	33.3	0	4.6	16.9	$2.69 \pm 0.18$	0.1258	PowerLaw
2FGL J1844.3+1548	281.1	15.8	46.3	8.7	4	12.5	29.8	$2.43 \pm 0.08$	0.0403	PowerLaw
2FGL J2004.6+7004	301.2	70.1	102.9	19.5	0	9.5	36.8	$1.97 \pm 0.11$	0.0368	PowerLaw
2FGL J2115.4+1213	318.9	12.2	62.6	-24.5	0	5.1	25.3	$2.38 \pm 0.19$	0.0800	PowerLaw
2FGL J2351.6-7558	357.9	-76.0	307.7	-40.6	0	4.1	20.8	$1.92 \pm 0.19$	0.0702	PowerLaw

NOTE. — The table provides detailed information about the unassociated 2FGL point sources we have identified with at least one 100-140 GeV photon within  $0.15/0.3^\circ$  for FRONT/BACK events. The first column is the 2FGL catalog name in the format 2FGL JHHMM.m+DDMM, where 'c' indicates that the source is considered to be potentially confused with Galactic diffuse emission. The second/third column are Right Ascension (J2000) and Declination (J2000). The fourth and fifth column are Galactic Longitude and Galactic Latitude. The sixth column is the flag parameter which indicate possible issues noted in detection or characterization of the source. Sources having no flags raised with value 0 are those without potential problems. The seventh column is the variability index, defined as the test statistic for the hypothesis that monthly averages of the source flux vary relative to the null hypothesis of constant flux. The TS is distributed as  $\chi^2$  with 23 degrees of freedom, so a value greater than 41.64 indicates a  $> 99\%$  chance of being a variable source, and we have removed these sources from our analysis. The eighth column shows the best fit for the photon number power-law index (for logarithmic parabola spectra it is index at the Pivot Energy) derived from the likelihood analysis for 100 MeV-100 GeV. The ninth column shows the average of semimajor/semiminor axis of the error ellipse at 68% confidence. Source detection significance in Gaussian  $\sigma$  units is shown in the tenth column, which is derived from the likelihood Test Statistic for 100 MeV-100 GeV analysis. The eleventh column shows the best fit form of the spectral type. We note that only three sources have logarithmic parabolic spectral shape (two of them are marked with potentially confused with Galactic diffuse emission). Detailed explanation of parameters listed in this table can be found in Nolan et al. (2012).

## APPENDIX

We show the same energy spectrum as in Figure 1 but with high incidence angle events only with  $\theta > 40^\circ$  in Figure 9. In Figure 10, we show that the 111 GeV and 129 GeV lines do not appear in the SOURCE minus ULTRACLEAN events, i.e. cosmic ray contamination is not a plausible explanation for the line emission. In Figure 11 and Figure 12 we show the unassociated/associated point sources by matching with LAT events of different energy range. We also compare with distributions of all the unassociated/associated sources. Selection effect is plausible explanation for the spatial distribution of selected unassociated sources shown in Figure 8.

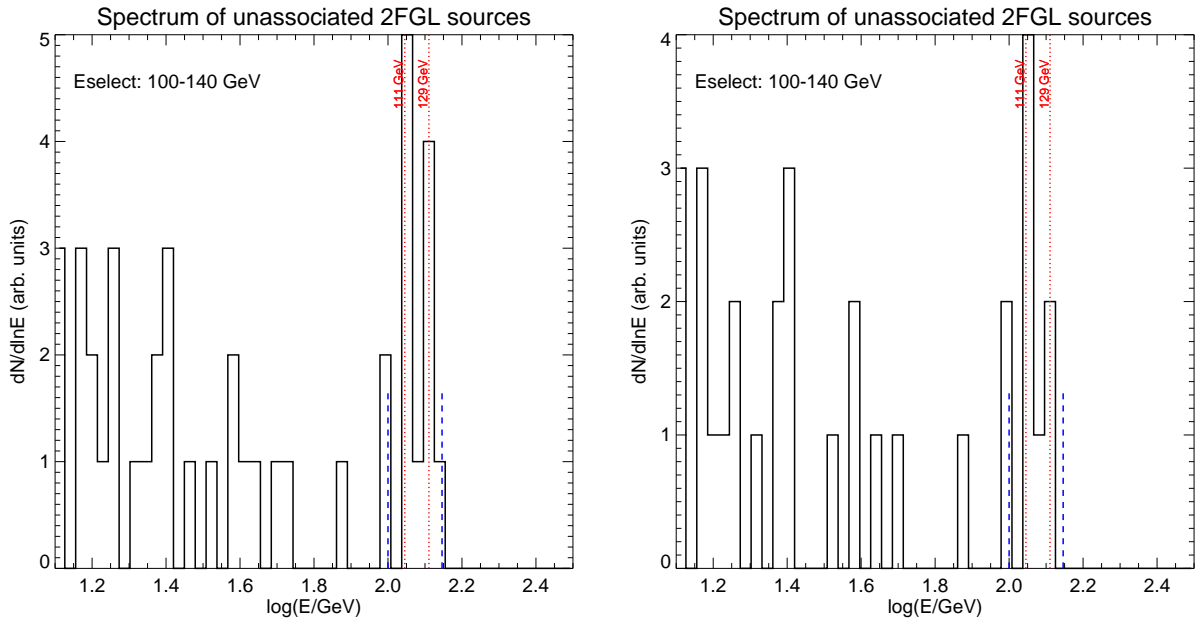


FIG. 9.— Same as the upper left panel of Figure 1, but using only events with high incidence angle  $\theta > 40^\circ$  which has better energy resolution to reveal the energy spectrum of unassociated 2FGL catalog. We found two gamma-ray line emission on 111 GeV and 129 GeV.

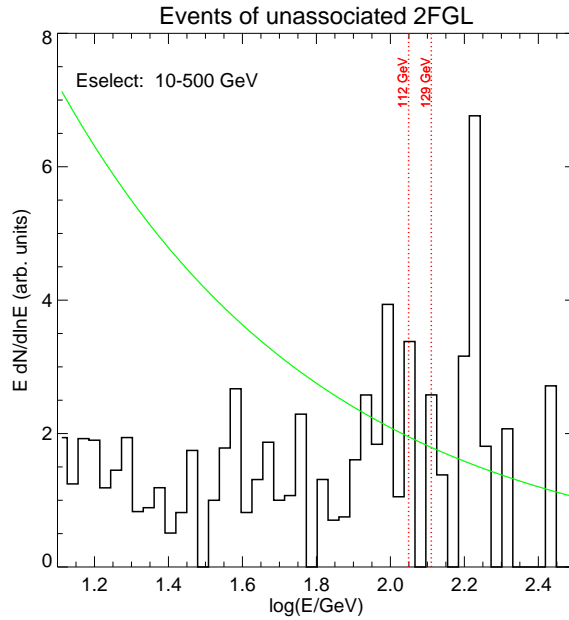


FIG. 10.— Same as the upper left panel of Figure 1, but using only events belongs to SOURCE class but *not* to ULTRACLEAN event. This selected set of events are dominated by cosmic ray events. We found no significant gamma-ray line emission on 111 GeV and 129 GeV ( $0.47\sigma$  with background estimation using 100-500 GeV data).

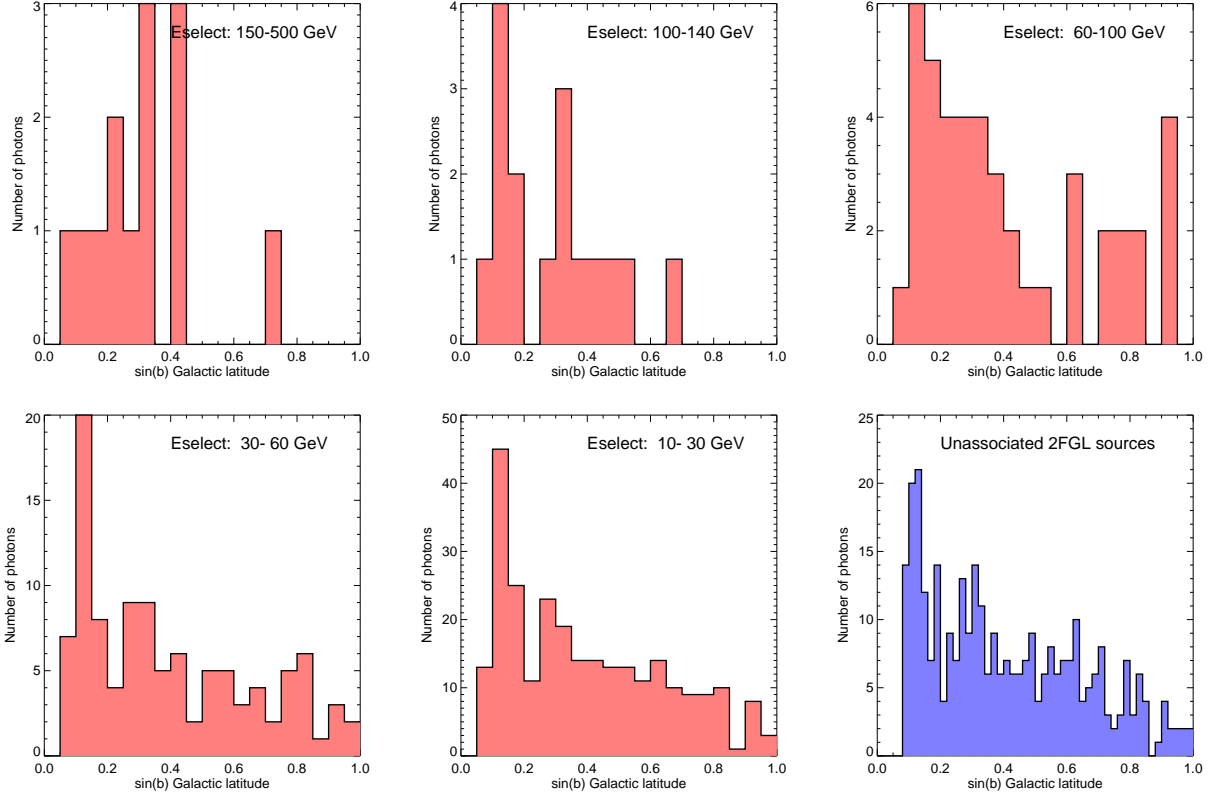


FIG. 11.— The distribution of unassociated 2FGL sources selected by matching with LAT photons of different energy range. The panels from the upper left to lower right are for 150-500 GeV, 100-140 GeV, 60-100 GeV, 30-60 GeV, and 10-30 GeV, and for comparison all unassociated sources with  $|b| > 5^\circ$  and variability index  $< 41.64$ .

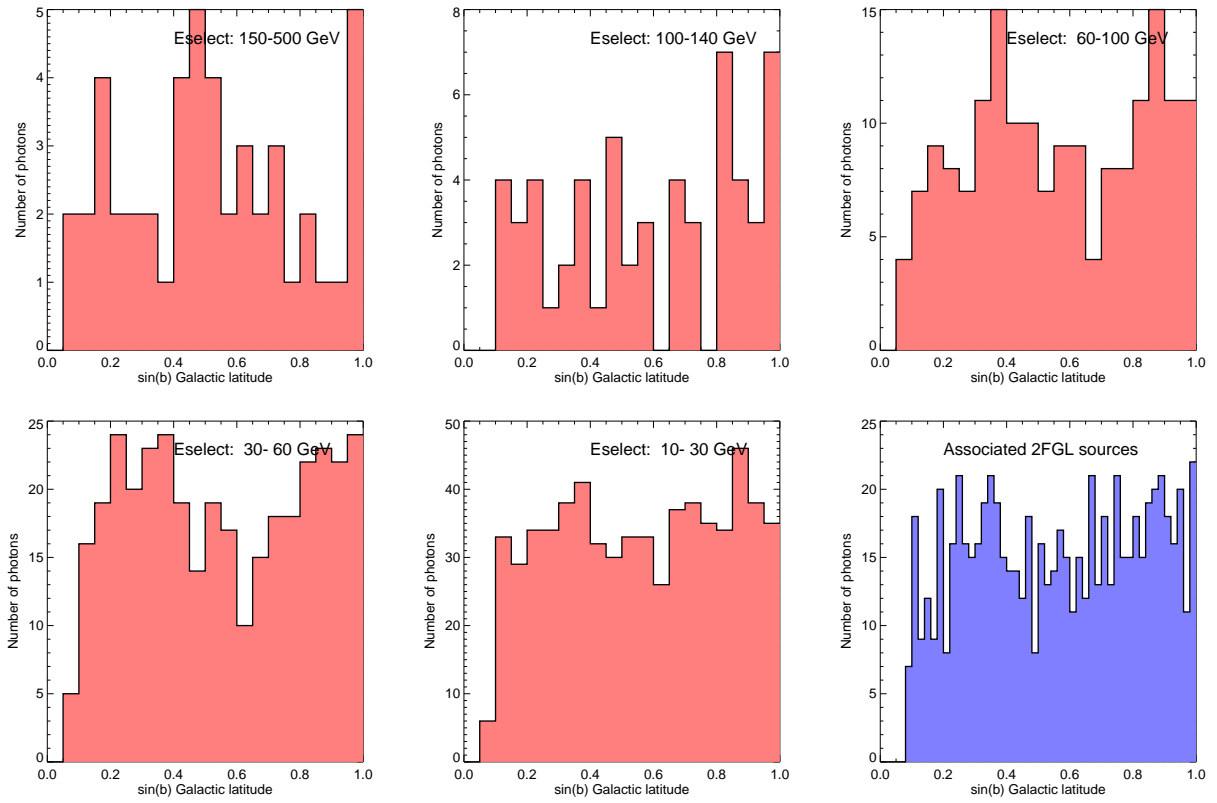


FIG. 12.— The same as Figure 11, but for the associated 2FGL sources.